Article | Received 31 December 2025; Revised 24 May 2026; Accepted 16 June 2026; Published 25 June 2026
https://doi.org/10.55092/esp20260004

Analysis of dementia EEG signals using empirical mode decomposition variants and deep learning †

Yahya Oguzhan Senol[1], Aydin Akan[1,*] and Ozlem Karabiber Cura[2]

[1] Department of Electrical and Electronics Engineering, Izmir University of Economics, Izmir, Turkey
[2] Department of Biomedical Engineering, Izmir Katip Celebi University, Izmir, Turkey

† This work is an extended version of the paper presented at 2025 Medical Technologies Congress TIPTEKNO'25.

* Correspondence author; E-mail: akan.aydin@ieu.edu.tr.

Highlights:

- Use advanced signal decomposition methods to analyze EEG signals.
- Obtain spatial information using Topo-maps.
- Compare CNN architectures to evaluate the performance.

Abstract: In recent years, Alzheimer's dementia (AD) is the most common neurological condition caused by electrical activity changes in the human brain. The diagnosis of AD can be provided by using medical devices such as electroencephalography (EEG). In this study, EEG signals of AD patients and healthy control subjects were analyzed. Advanced signal decomposition methods, which are empirical mode decomposition (EMD) and ensemble empirical mode decomposition (EEMD), were used to further investigate EEG signals. The first three intrinsic mode functions (IMFs) were obtained using the EMD and EEMD methods. Spectral and time-domain features were extracted from IMFs and raw EEG signals. Then, topographical heat maps were generated from these features. Topographic Feature Map (Topo-map) were classified using a two-dimensional convolutional neural network (2D-CNN). Different CNN architectures were compared in terms of performance, including EfficientNet-b0, Resnet-50, and Resnet-18. The experimental results demonstrate that the proposed approach effectively captures the spatial and spectral characteristics of EEG signals associated with Alzheimer's disease. 95.98% classification accuracy was achieved with the EfficienNet-b0 architecture.

Keywords: Alzheimer dementia (AD); electroencephalography (EEG); empirical mode decomposition (EMD); ensemble empirical mode decomposition; convolutional neural network (CNN); intrinsic mode functions (IMFs)

1. Introduction

Dementia refers to the loss of brain functions. Alzheimer's dementia (AD) is the most common type of dementia. AD is an advancing neurological illness and a widespread public health issue. Its effects include cognitive decline, memory loss, and behavioral abnormalities [1]. AD accounts for 65% to 80% of all dementia cases and is known as one of the leading causes of death in adults over the age of 65 [2]. AD does not currently have a cure, and medical treatments can only slow the progression of the condition. People can learn about AD and make plans for future needs when the disease is diagnosed early. So, diagnosis is crucial. For diagnostic purposes, machine learning methods are considered more advanced than traditional approaches such as psychological assessments, as they offer faster processing with the help of modern GPU technology.

Numerous medical techniques can be used to diagnose AD and monitor how well a patient is responding to treatment. Positron Emission Tomography (PET) and Magnetic Resonance Imaging (MRI) are performed to detect symptoms associated with AD [3]. Also, electroencephalography (EEG) is another technique that uses electrodes applied to the scalp to record electrical impulses from the brain [4]. EEG shows the electrical activity in the brain as waves with different shapes, frequencies, and amplitudes. While techniques like MRI and PET offer high spatial resolution, they may miss certain abnormalities due to their limited temporal resolution. In contrast, electroencephalography EEG is superior in terms of temporal resolution, cost-effectiveness, and availability [5].

There are many studies in the literature for the classification of EEG signals. In some of them, features from EEG signals like Tsallis entropy [6], multivariate multiscale weighted permutation entropy [7], permutation Jaccard distance [8], and Fuzzy Entropy (FuzzyEn) [9] are used to distinguish the patient and control group. Apart from calculating many features from EEG signals, signal decomposition approaches with the help of machine learning are also used for AD classification. Some of these approaches are Discrete Wavelet Transform (DWT), intrinsic time-scale decomposition (ITD), empirical mode decomposition (EMD), and ensemble empirical mode decomposition (EEMD). DWT analyzes signals in both the time and frequency domains, making it suitable for non-stationary signals such as EEG. It decomposes the signal into different frequency bands by separating it into approximation (low-frequency) and detail (high-frequency) coefficients. In the study using detail and approximation coefficients of DWT with the machine learning methods that are decision tree (DT), k-nearest neighbor (kNN), support vector machine (SVM), and random forest (RF), 95.2% classification accuracy was achieved [10]. In another study about the classification of AD patients and healthy subjects, combining spectral features and DWT features, 94% classification accuracy was achieved [11].

Studies are using intrinsic time-scale decomposition (ITD) to classify between AD patients and healthy control subjects. ITD is suitable for nonlinear and non-stationary signals like EEG. It decomposes the signal into proper rotation components (PRCs). In the study of classification of AD, using PRCs using the Short-Time Fourier Transform (STFT). These spectrograms were then used to classify AD patients and control subjects via a two-dimensional convolutional neural network (2D-CNN), achieving a test accuracy of 98.6% [12].

EMD and EEMD are used especially to analyze nonlinear and non-stationary signals like EEG. EMD decomposes the signal into intrinsic mode functions (IMFs). Each IMF represents the part of the signal that contains a certain oscillation. When the IMFs are added together, the original signal is

reconstructed. Sometimes, similar oscillations can be found in different IMFs, and different oscillations can be found in the same IMF. To prevent this issue, the EEMD method is utilized. EMD and EEMD are also used in studies for the classification of AD, similar to DWT and ITD. In a study, segmented EEG signals were decomposed into the first seven IMFs with the EMD and EEMD methods. Then, spectral and time-domain features were extracted from these IMFs and used to classify AD patients and healthy control subjects using machine learning methods such as DT, kNN, SVM and RF [10]. In that study, 91.8% classification accuracy was obtained using EMD, and 94.1% classification accuracy was obtained using EEMD. Another study benefited from DWT and EMD for feature extraction, and SVM, k-NN and Linear Discriminant Analysis (LDA) for classification [13]. Their study achieved 97.64% accuracy using k-fold cross-validation and 81.08% accuracy using leave-one-subject-out (LOSO) validation.

Recent advances in deep learning have further expanded the landscape of EEG-based AD classification. Transformer-based architectures and attention mechanisms have been applied to EEG signals, enabling models to capture long-range temporal dependencies that are disrupted in AD. Alvi *et al.* [14] proposed a temporal convolutional network combined with a self-attention mechanism for EEG-based dementia classification, achieving competitive accuracy while reducing reliance on manual feature engineering. Similarly, Fiscon *et al.* [15] demonstrated that graph neural networks applied to EEG connectivity matrices can effectively distinguish AD patients from healthy controls, highlighting the role of altered brain network topology in the disease. In the area of multi-channel EEG representation learning, Ieracitano *et al.* [16] explored the use of statistical frequency-domain features fed into a deep convolutional neural network, reporting strong classification performance on a multi-class AD staging task. More recently, Wan *et al.* [17] applied a hybrid convolutional-recurrent architecture to EEG spectrograms for AD detection, demonstrating the benefit of combining spatial and temporal feature extraction in a unified deep learning framework. These recent works collectively motivate the use of spatially meaningful representations—such as the topographic maps employed in the present study—as inputs to CNN-based classifiers.

In this study, noise was removed from the EEG signals of AD patients and control subjects using a Butterworth filter. The filtered signals were then segmented into 5-second and 1-minute intervals. EMD was applied to each segment, and the first three IMFs were extracted (the rationale for selecting the first three IMFs is discussed in Section 2.3). Also, EEMD was applied to just 1-minute segments, and the first three IMFs were extracted. Only spectral features were extracted from the IMFs obtained with EEMD, and time-domain and spectral features were extracted from both the IMFs obtained with EMD and the raw EEG signals and were subsequently transformed into Topo-map. These RGB Topo-map images were used to classify AD patients and control subjects using a two-dimensional convolutional neural network (2D-CNN) architecture, including ResNet50, EfficientNet-b0, and ResNet-18. The classification process is implemented in the MATLAB environment.

2. Methods

In this section, data set used in this study will be introduced. Preprocessing of EEG signals and segmentation of EEG signals will be shown. EMD and EEMD, two of the signal decomposition approaches, will be examined. Time and spectral features that were extracted from IMFs and EEG signal itself, will be discussed. Lastly, topographic heat map generation and 2D CNN architectures will be analyzed.

2.1. AD data set

EEG data used in this study were obtained from patients evaluated at the dementia clinic of the Neurology Department, Izmir Katip Celebi University Faculty of Medicine. These patients were diagnosed with early-stage Alzheimer's disease by diagnostic tests and neuroimaging. EEG signals were recorded for 15 AD patients (30 minutes for each patient). Their average age is 64. 7 of them are males, and 8 of them are females. EEG recording was done for each patient from 19 channels at 200 Hz sampling frequency in the resting state with the eyes closed. EEG signals were recorded only, and different biological signals like ECG and EOG were not collected during the recording process. Recordings were obtained from 19 scalp electrodes placed according to the International 10–20 system at the following positions: Fp1, F7, T3, T5, O1, O2, T6, T4, F8, Fp2, F3, Fz, F4, C3, Cz, C4, P3, Pz, and P4 as shown in Figure 1. For comparison, EEG data were also collected from 11 cognitively healthy controls (HC), age-matched control subjects using the same recording system and electrode placement. 6 of them are males, and 5 of them are females. Their average age is 57.

2.2. Preprocessing and segmentation of EEG signals

Firstly, at the preprocessing stage, a Butterworth band pass filter was used for all channels of AD and HC. A pass band of 0.5–40 Hz is applied to all channels to eliminate unwanted electrical noise and some artifacts, such as eye-blinking and muscle activity of individuals.

Later, filtered EEG signals were divided into non-overlapping 5-second and 1-minute segment durations separately. For the HC group, there were 11 individuals. For each individual, there were 19 channels. So, there were 19 × 11 × 30 = 6270 EEG segments for the control group in the 1-minute case. EEG signals were 30 minutes long, and EEG signals were recorded at a 200 Hz sampling frequency. Each 1-minute segment has 12,000 samples. EEG signals have approximately 360,000 samples per channel. In order to have a balanced data set, 19 × 15 × 22 = 6270 segments were generated for AD in 1 min case. So, 12,000 × 22 = 264,000 samples were used for each AD patient's channel. 360,000 – 264,000 = 96,000 samples which means 96,000 / 12,000 = 8 segments per channel for each AD patient in 1 minute case were not used to have balanced data set between AD and HC in 1 min case. So, a total of 19 × 15 × 8 = 2280 segments were not used for AD in 1 min case. Also, the same structure with minor changes occurred in the 5-second case. 19 × 11 × 360 = 75,240 segments were generated for controls, and 19 × 15 × 264 =75,240 segments were generated for AD to have balanced data sets in the 5s case. 1000 × 264 = 264,000 samples were used for each patient's channel. 360,000 – 264,000 = 96,000 samples, so 96,000 / 1000 = 96 segments per channel for each AD were not used to have a balanced data set between AD and HC in the 5 s case. Thus, a total of 19 × 15 × 96 = 27,360 segments were not used for AD in 1 min case.

2.3. EMD

In this study, EMD is used. EMD is a signal decomposition method to have ability to process non-linear and non-stationary signals. EMD provides IMFs and a residual. A higher mode number contains smaller frequencies. The sum of all modes and the remaining residual resembles the original signal as given in equation 1. In this study, the first three IMFs were selected for analysis. In EMD, the lower-indexed IMFs

(IMF1, IMF2, IMF3) correspond to the highest-frequency oscillatory components of the signal. Although AD is primarily associated with increased low-frequency (delta and theta) activity, the higher-frequency IMFs also carry diagnostically relevant information: high-frequency gamma and beta oscillations are known to be disrupted in AD due to impaired cortical synchronization [1,5]. Moreover, the early IMFs tend to exhibit the highest signal energy and signal-to-noise ratio, making them the most robust for feature extraction. In addition, selecting only three IMFs substantially reduces the computational burden of feature extraction and Topo-map generation. Higher-order IMF combinations will be explored in future work to determine optimal IMF subsets for classification.

$$f(t) = \sum_{i} imf_i(t) + res(t) \quad (1)$$

The algorithm for EMD is shown below.

Algorithm 1 Empirical Mode Decomposition (EMD)

1. Find local extrema (local minima and local maxima) of the signal $f(t)$.
2. Fit maxima and minima to an individual envelope. Calculate upper envelope $E_{upp}(t)$, and lower envelope $E_{low}(t)$ using cubic spline interpolation.
3. Determine the average of $E_{upp}(t)$ and $E_{low}(t)$.

$$E_{mean}(t) = \frac{(E_{upp}(t) + E_{low}(t))}{2} \quad (2)$$

4. Determine residual $res(t) = f(t) - E_{mean}(t)$ if $res(t)$ satisfies the condition of IMF, $res(t) = IMF_1(t)$ else go to step 1 and repeat every process using $res(t)$ instead of $f(t)$.
5. After getting $IMF_1(t)$, calculate the residue $res_1(t) = f(t) - IMF_1(t)$. If this residue is not monotonic, return to step 1 and calculate a new IMF from $res_1(t)$.

2.4. EEMD

In this study, Ensemble EMD, an improved variant of EMD, is also utilized. EEMD is aimed to fix the so called “mode mixing problem” occurred in EMD. EEMD enhances the EMD process by reducing mode mixing. In the mode mixing problem, a single IMF contains multiple oscillatory modes or a single mode residing in multiple IMFs. The EEMD approach is shown below.

(1) Add ensembles of white Gaussian noise $w_n(t)$ to the input signal $f(t)$.

$$f_n(t) = w_n(t) + f(t) \quad (3)$$

(2) Decomposition of the noisy data $f_n(t)$ with the standard EMD

(3) Taking the ensemble mean of all resulting IMFs

$$imf(t) = \frac{1}{N}\sum_{n=1}^{N} imf_n(t) \quad (4)$$

2.5. Feature extraction

Time-domain and spectral features were extracted for each EEG segment and their corresponding IMFs obtained with EMD, for both HC and AD. Only spectral features were extracted for 1 min IMFs obtained with EEMD for both HC and AD. Time-domain features are activity, mobility, complexity, skewness, and kurtosis. These time-domain features give valuable information about the signal to distinguish between HC and AD. For example, activity provides information about signal power. Mobility and complexity give information about the frequency characteristics of a signal. Skewness indicates whether a signal's distribution is symmetric or not. Kurtosis provides information about the peak and outliers of the signal distribution. Spectral features are total power, spectral entropy, first, second, and third moments. These features give important information about the signal to discriminate between HC and AD, too. Total power represents total frequency content. It is the sum of the power spectra of all frequency components. Spectral entropy measures the randomness and entropy of frequency components. Higher-order spectral (HOS) moments capture the shape of the power spectrum. All time-domain and spectral feature formulas are in Table 1. In these formulas, $x[n]$ is the EEG signal or IMFs. N is the size of the EEG signal or IMFs. $\mu = \frac{1}{N}\sum_{n=1}^{N} x[n]$ is the mean value. $w_k = \frac{2\pi}{N}k$; $S(w_k) = \frac{1}{N}|X(w_k)|^2$ is the power spectral density. $X(w_k)$ is the Discrete Fourier Transform of $x[n]$. $P(w_k) = \frac{S(w_k)}{Total\ Power}$ is the normalized power spectral density.

Table 1. Time-domain and spectral features and their formulations.

Time and Spectral Features	Formulation	
Activity	$\sigma^2 = variance(X[n]) = \frac{1}{N}\sum_{n=0}^{N-1}(x[n]-\mu)^2$	(5)
Mobility	$\sqrt{\frac{variance\left(\frac{dx[n]}{dn}\right)}{variance(x[n])}}$	(6)
Complexity	$\frac{\text{mobility}\left(\frac{dx[n]}{dn}\right)}{\text{mobility}(x[n])}$	(7)
Skewness	$\frac{1}{N}\times\frac{\frac{1}{N}\sum_{n=1}^{N}(x[n]-\mu)^3}{\sigma^3}$	(8)
Kurtosis	$\frac{1}{N}\times\frac{\frac{1}{N}\sum_{n=1}^{N}(x[n]-\mu)^4}{\sigma^4}$	(9)
Total Power	$\sum_{k=0}^{N-1} S(w_k)$	(10)
Spectral Entropy	$\sum_{k=0}^{N-1} P(w_k)\times log_2 P(w_k)$	(11)
HOS Moments	$-\sum_{k=0}^{N-1} {w_k}^j \times S(w_k), j = 1,2,3$	(12)

2.6. Topographic heat map generation

After the feature extraction process, Topographic Feature Maps (Topo-map) were generated for time and spectral features of 1 min and 5 s segments of EEG signals and IMFs. Matlab's EEGLAB toolbox was used for it. The Topoplot function, defined in EEGLAB, was used to obtain Topo-maps. In order to get visually distinctive images, appropriate transformations are made on the time-domain and spectral features. To generate a Topo-map, the time-domain or spectral feature value in each corresponding segment of 19 channels of an AD or a HC was used. For example, activity values, one of the time features, of the third segments of each channel were used to plot activity topomap for IMF1 of an AD. There are 30 Topo-map images for a feature, extracted from 1 min EEG segment of a control. There are 11 controls and 10 features (5 time-domain and 5 spectral). Thus, 30 × 11 × 10 = 3300 images were generated for that case. 3300 × 3 = 9900 images were generated for 1 min IMFs (IMF1, IMF2, and IMF3) of controls. There are 22 Topo-map images for a feature, extracted from 1 min EEG segment of an AD. There are 15 AD and 10 features (5 time-domain and 5 spectral). Thus, 22 × 15 × 10 = 3300 images were generated for that case. 3300 × 3 = 9900 images were generated for 1 min IMFs (IMF1, IMF2, and IMF3) of AD. There are 360 Topo-map images for a feature, extracted from a 5 s EEG segment of a control. There are 11 controls and 10 features (5 time-domain and 5 spectral). Thus, 360 × 11 × 10 = 39600 images were generated for that case. 39,600 × 3 = 118,800 images were generated for 5 s IMFs (IMF1, IMF2, and IMF3) of controls. There are 264 Topo-map images for a feature, extracted from 5 s EEG segment of an AD. There are 15 AD and 10 features (5 time-domain and 5 spectral). Thus, 264 × 15 × 10 = 39,600 images were generated for that case. 39,600 × 3 = 118,800 images were generated for 5 s IMFs (IMF1, IMF2, and IMF3) of AD. A total of 118,800 × 2 + 39,600 × 2 + 9900 × 2 + 3300 × 2 = 343,200 images were generated. Also, 4950 Topo-map for AD and 4950 Topo-map for controls were generated using spectral features extracted from 1 min IMFs (IMF1, IMF2, and IMF3) obtained with EEMD method.

Topo-map give information about spatial distribution of brain activity across EEG channels for corresponding features. With Topo-map, it is possible to observe which feature is more dominant in which channel for that signal (IMFs or EEG). Figure 1 shows Topo-map of spectral entropy (one of the spectral features) of the first three IMFs obtained with EMD, extracted from 1 min segments of an AD patient. Figure 2 shows Topo-map of spectral entropy of the first three IMFs obtained with EMD, extracted from 1 min segments of a control subject. In these figures, crimson corresponds to higher values for spectral entropy feature, whereas light blue corresponds to lower values for spectral entropy feature. It can be observed from the figures that IMF1 spectral entropy Topo-map, for an AD from 1 min segments, is more dominant than IMF2 and IMF3 spectral entropy Topo-maps for C3 and FZ channels. Also, it can be observed from figures that red intensity of spectral entropy Topo-maps, for a control from 1 min segments, between P4 to C4 channels is decreasing from IMF1 to IMF3.

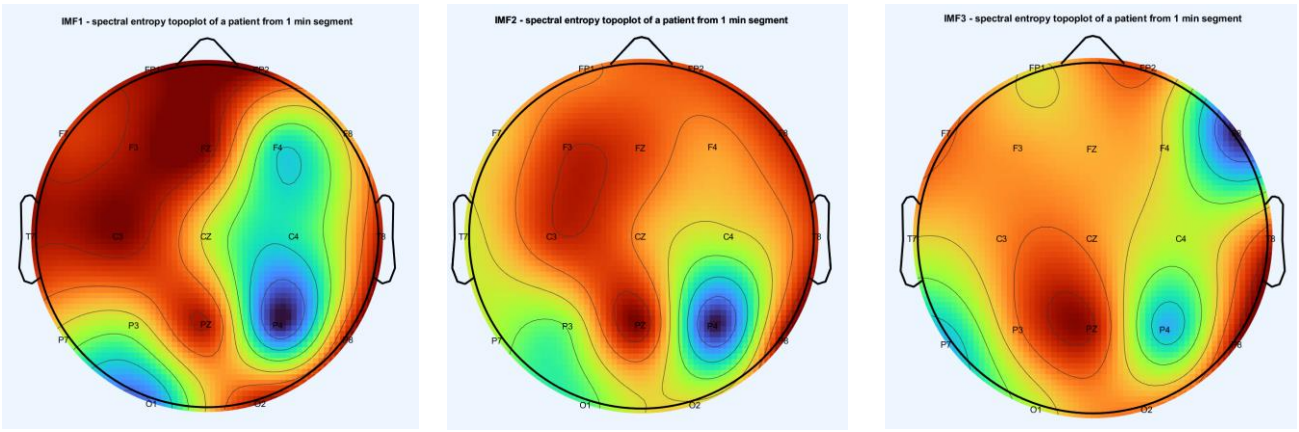

(a) (b) (c)

Figure 1. Spectral entropy Topo-maps of an AD patient from 1 min EEG segment: **(a)** IMF1; **(b)** IMF2; **(c)** IMF3.

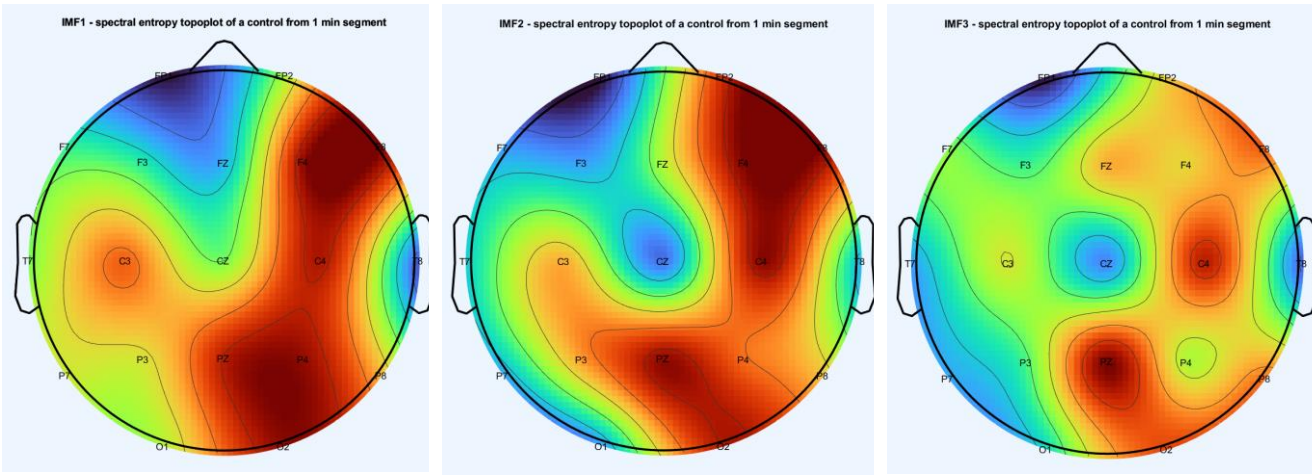

(a) (b) (c)

Figure 2. Spectral entropy Topo-maps of a control subject from 1 min EEG segment: **(a)** IMF1; **(b)** IMF2; **(c)** IMF3.

2.7. CNN architectures for classification

Topo-maps for spectral and time features from IMFs and EEG signals were used to classify AD and HC with deep learning. A 2D CNN was used for the classification of images. In this section, CNN architectures used in this study will be introduced.

2.7.1. ResNet-50

ResNet-50 was introduced in 2015 [18]. It is a pre-trained deep neural network and a CNN architecture. It consists of 50 layers. It accepts images with a size of 224 × 224 × 3. Because of that, topo images are resized to 224 × 224 × 3. It is used for the classification of images. In this study, classification of Topo-map images belonging to HC and AD was done with the help of ResNet-50. ResNet-50 is designed for classifying 1000 classes. In the proposed study, there are only 2 classes (AD and HC). Thus, the last three layers of ResNet-50 were removed. These are fc1000 (fully connected layer), fc1000_softmax

(softmax layer), and ClassificationLayer_fc1000 (classification layer). 3 new layers were added with suitable changes for two class classification. Training options are adjusted for ResNet-50. Maximum epoch is set to 10. Learning Rate is set to 0.0001. Adaptive Moment Estimation (Adam) optimization is used.

2.7.2. ResNet-18

ResNet-18 consists of 18 convolutional layers. It is lighter than ResNet-50. ResNet-18 is advantageous because of its ease of training, good accuracy, and low computational cost. First layer of ResNet-18 is data, which is an Image Input Layer in Matlab. ImageInput accepts images with a size of 224 × 224 × 3. Because of that, Topo-map images are resized to 224 × 224 × 3. ResNet-18 is designed for classifying 1000 classes like ResNet-50. 2 layers, which are fc1000 (fully connected layer) and classificationLayer_predictions (classification layer), are removed from the ResNet-18 CNN architecture. New 2-layer models suitable for two-class classification are replaced. The maximum epoch is set to 10. Learning Rate is set to 0.0001. Adam optimization is used.

2.7.3. EfficientNet-b0

EfficientNet-b0 was introduced in 2019 [19]. It has approximately 82 layers. It is used for medical image classification tasks. Its input layer accepts images with a size of 224 × 224 × 3, too. It is slightly slower on the CPU. It is designed for classifying 1000 classes, too. Because of that, efficientnet-b0|model|head|dense|MatMul (fully connected layer), and classification (classification layer) layers are removed, and new layers are replaced for 2-class classification, like ResNet-50 and ResNet-18. Maximum epoch is set to 10. Learning Rate is set to 0.0001. Stochastic gradient descent with momentum (sgdm) optimization is used.

3. Results

Until there, 5 s and 1 min EEG segments were obtained from AD and HC. EMD was used to get the first three IMFs for these segments, and EEMD was used to get the first three IMFs for 1 min segments. Time-domain and spectral features were extracted from the EEG signal and IMFs obtained with EMD. Only spectral features were extracted from IMFs obtained with EEMD. Then Topo-maps were generated using these features for AD and HC. In this chapter of the study, classification between AD and HC were performed for different datasets with ResNet-50, ResNet-18, and EfficientNet-b0. Generated Topo-maps using time-domain features of 1 min and 5 s IMFs, obtained with EMD, of AD and time-domain features of 1 min and 5 s IMFs, obtained with EMD, of HC were classified. Also, generated Topo-maps using spectral features of 1 min and 5 s IMFs, obtained with EMD, of AD and spectral features of 1 min and 5 s IMFs, obtained with EMD, of HC were classified. These classifications were performed with 1 min and 5 s EEG for both time-domain feature Topo-maps and spectral feature Topo-maps of AD and HC, too. Finally, generated Topo-maps using spectral features of 1 min IMFs, obtained with EEMD, of AD and spectral features of 1 min IMFs, obtained with EEMD, of HC were classified. To prevent data leakage, contour lines and electrode names were extracted from Topo-map. As an example, an image that is used in classification is shown in Figure 3.

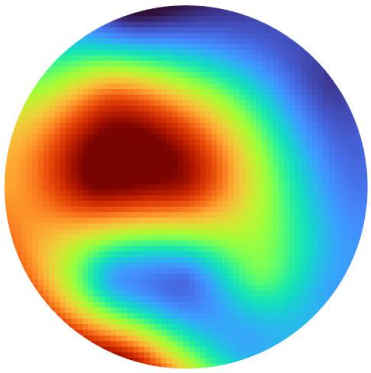

Figure 3. Example image used in classification.

3.1. Performance metrics

In order to evaluate the performance, a confusion matrix was used. The confusion matrix is 2 × 2, because two classes (AD and HC) exist in this study. True positive (TP) corresponds to the number of AD Topo-maps correctly detected as AD. True negative (TN) corresponds to the number of HC Topo-maps correctly detected as HC. False positive (FP) corresponds to the number of HC Topo-maps incorrectly detected as AD. False negative (FN) corresponds to the number of AD Topo-maps incorrectly detected as HC. From these values, accuracy (ACC), sensitivity (SEN), specificity (SPE), precision (PRE), and F1 score are obtained. There are formulas for them in Table 2. In this study, these performance metrics were used.

Table 2. Performance metrics and their formulations.

Performance Metrics	Formulation	
Accuracy	$\frac{(TP+TN)}{(TP+FN+TN+FP)}$	(13)
Sensitivity	$\frac{TP}{(TP+FN)}$	(14)
Specificity	$\frac{TN}{(TN+FP)}$	(15)
Precision	$\frac{TP}{(TP+FP)}$	(16)
F1-score	$2\times\frac{(precision\times sensitivity)}{(precision+sensitivity)}$	(17)

3.2. Classification results

In the previous chapter, the number of Topo-maps for 1 min was examined. There was a total of 9900 Topo-maps for 1 min IMFs of AD, and 9900 Topo-maps for 1 min IMFs of HC. Half of Topo-maps for

1 min IMFs of AD were Topo-maps for spectral features, and other half were Topo-maps for time features. Same numbers are also valid for 1 min IMFs of HC. There was a total of 3300 Topo-maps for 1 min EEG of AD, and 3300 Topo-maps for 1 min EEG of HC. Half of Topo-maps for 1 min EEG of AD were Topo-maps for spectral features, and the other half were Topo-maps for time features. The same numbers are also valid for 1 min EEG of HC.

Likewise, in the previous chapter, the number of Topo-maps for 5 s was examined. There was a total of 118800 Topo-maps for 5 s IMFs of AD, and 118800 Topo-maps for 5 s IMFs of HC. Half of Topo-maps for 5 s IMFs of AD were Topo-maps for spectral features, and the other half were Topo-maps for time features. Same numbers are also valid for 5 s IMFs of HC. There was a total of 39,600 Topo-maps for 5 s EEG of AD, and 39,600 Topo-maps for 5 s EEG of HC. Half of Topo-maps for 5 s EEG of AD were Topo-maps for spectral features, and the other half were Topo-maps for time features. Same numbers are also valid for 5 s EEG of HC.

The number of Topo-maps for all these cases are shown in Figures 4 and 5.

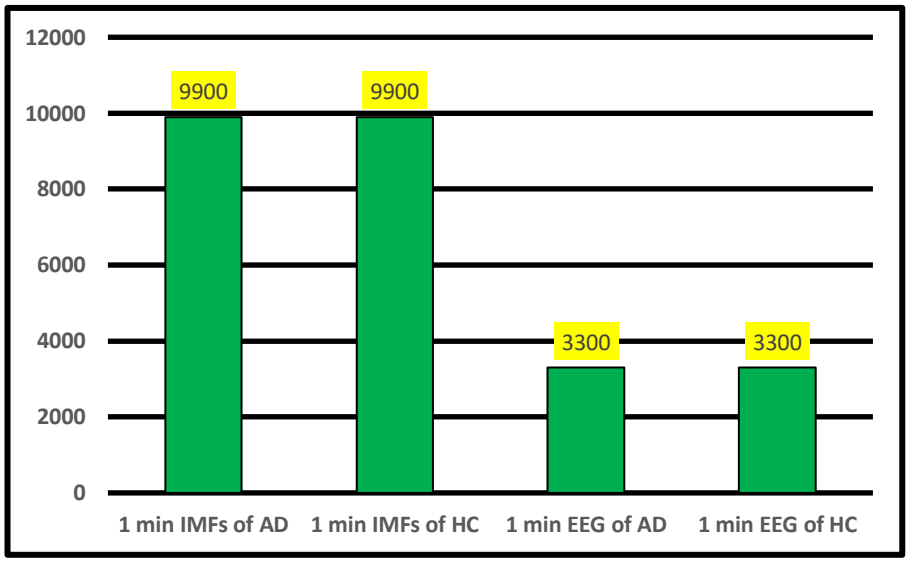

Figure 4. Number of Topo-maps for 1 min.

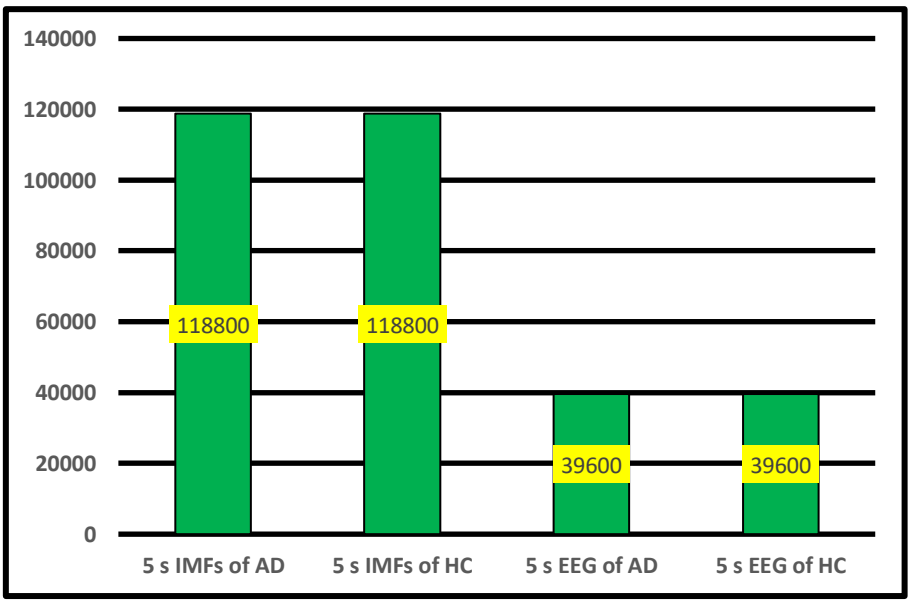

Figure 5. Number of Topo-maps for 5 s.

In this study, there are a total of 9 cases for 1-minute segment duration of spectral features Topo-map. Each CNN architecture has 3 cases. On the other hand, there are a total of 6 cases for 1-minute segment duration of time features Topo-map, and each CNN architecture has 2 cases. In addition, for the 5-second segment duration, there are a total of 6 cases for the time-domain features and another six cases for the spectral-domain features' Topo-map. For each case, the data was split into 80% for training and 20% for validation using a random image-level split. It should be noted that this splitting strategy does not enforce subject independence; images from the same subject may appear in both training and validation sets. A subject-independent evaluation (e.g., leave-one-subject-out cross-validation) would provide a stricter assessment of generalizability and is recommended for future work. Performance metrics, which are validation ACC, SEN, SPE, PRE, and F1 score, are examined. Classification results for the 1-minute segment duration and the 5-second segment duration were given in Table 3 and Table 4, respectively.

From these tables, it can be observed that the classification results of 1 min cases were better than 5 s cases. Also, spectral features Topo-map give better results than time features Topo-map. In addition, spectral features Topo-map for a 1 min segment duration are best when we compare with other cases. Because of that, the EEMD method is beneficial for only spectral features Topo-map for 1 min segment duration to save computation time. The best accuracy value 95.98% was achieved with the EEG from the Efficient-b0 architecture. Although EEG gives higher performance from EMD and EEMD, we can observe that the accuracy of EEMD was very close to that of EEG, and even EEMD accuracy (% 95.60) was higher than EEG for the ResNet-50 network. So, the performance of EMD is increased with EEMD, which is a variant of the EMD method. If we compare CNN architectures, Efficient-b0 and ResNet-50 architectures give better results than ResNet-18. This can be expected, as ResNet-18 is a more basic architecture compared to the others.

Table 3. Performance evaluation results of CS and AD EEG classification obtained using spectral and temporal features Topo-map for 1min segment duration.

	CNN Architectures	Method	Validation ACC	SEN	SPE	PRE	F1-Score
Spectral Features	ResNet-50	EEG	0.9474	0.9606	0.9292	0.9491	0.9548
		EMD	0.9271	0.9535	0.891	0.9228	0.9379
		EEMD	**0.956**	0.9569	0.9551	0.955	0.9559
	ResNet-18	EEG	0.9234	0.8967	0.9595	0.9676	0.9308
		EMD	0.9166	0.9303	0.8979	0.9255	0.9279
		EEMD	0.9228	0.9138	0.9316	0.9301	0.9219
	EfficientNet-b0	EEG	**0.9598**	0.98	0.9324	0.9515	0.9655
		EMD	0.9154	0.921	0.9077	0.9315	0.9263
		EEMD	0.9366	0.9497	0.9235	0.9251	0.9372
Temporal Features	ResNet-50	EEG	0.8336	0.8967	0.7754	0.7866	0.838
		EMD	0.8	0.8185	0.7816	0.7885	0.8032
	ResNet-18	EEG	0.8352	0.79	0.8769	0.8556	0.8215
		EMD	0.7215	0.6182	0.8245	0.7784	0.6891
	EfficientNet-b0	EEG	0.824	0.84	0.8092	0.8029	0.8208
		EMD	0.7494	0.7528	0.7459	0.7467	0.7497

Table 4. Performance evaluation results of CS and AD EEG classification obtained using spectral and temporal features Topo-map for 5s segment duration.

	CNN Architectures	Method	Validation ACC	SEN	SPE	PRE	F1-Score
Spectral Features	ResNet-50	EEG	**0.915**	0.9344	0.896	0.8984	0.916
		EMD	0.8402	0.8524	0.8273	0.8396	0.8459
	ResNet-18	EEG	0.8687	0.9046	0.8333	0.8474	0.8724
		EMD	0.8002	0.8184	0.7808	0.7987	0.8085
	EfficientNet-b0	EEG	0.8891	0.879	0.899	0.8955	0.8872
		EMD	0.787	0.8432	0.7273	0.7666	0.8031
Temporal Features	ResNet-50	EEG	0.7817	0.7764	0.7869	0.782	0.7792
		EMD	0.6775	0.6943	0.659	0.6923	0.6933
	ResNet-18	EEG	0.7389	0.7713	0.7071	0.7217	0.7457
		EMD	0.599	0.6781	0.5116	0.6054	0.6397
	EfficientNet-b0	EEG	0.7013	0.5836	0.8172	0.7587	0.6597
		EMD	0.596	0.4038	0.8084	0.6997	0.5121

To evaluate the effectiveness of the proposed method, a comparison with state-of-the-art studies in the literature utilizing similar datasets or methodologies is presented in Table 5.

Table 5. Comparison of the proposed method with state-of-the-art studies for AD detection.

Reference	Method/Features	Classifier	Accuracy
[10]	DWT + Statistical Features	Random Forest (RF)	95.20%
[11]	DWT + Statistical Features	SVM	94.00%
[14]	EMD / DWT + Hjorth Parameters	SVM	97.64%
[12]	ITD + Proper Rotation Components	2D-CNN	98.60%
Proposed Method	EEMD + Spectral Topo-maps	ResNet-50	95.60%
Proposed Method	Raw EEG + Spectral Topo-maps	EfficientNet-b0	95.98%

As observed in Table 5, the proposed method achieves competitive performance compared to existing studies. For instance, Bairagi [11] reported a classification accuracy of 94% using a combination of spectral and DWT features. Our study outperformed this result by achieving 95.98% accuracy using Deep Learning architectures to analyze Topo-maps, which provide a more robust representation by capturing the spatial distribution of brain activity. While Sen [12] reported a higher accuracy of 98.6% using ITD and spectrograms, our study offers a distinct advantage in terms of spatial interpretability. By using Topo-maps, we not only classify the subjects but also visualize the spatial distribution of brain activity (as shown in Figures 3 and 4), providing clinicians with valuable insights into which brain regions are most affected by AD.

4. Discussion

The results of this study, which extends our initial work presented at TIPTEKNO'25 [20], demonstrate that Topo-maps derived from EEG signals, combined with 2D-CNN architectures, can effectively

distinguish AD patients from HC. The highest classification accuracy of 95.98% was achieved using spectral feature Topo-maps of raw EEG with the EfficientNet-b0 architecture, and 95.60% was achieved with the EEMD-derived spectral Topo-maps using ResNet-50. These results are consistent with prior studies reporting high classification accuracies using deep learning on EEG-derived features [10–14].

From a neurophysiological perspective, the superiority of spectral features over time-domain features in this study aligns with established findings on EEG changes in AD. AD is widely associated with a "slowing" of EEG rhythms, characterized by decreased power in alpha (8–13 Hz) and beta (13–30 Hz) bands, and increased power in theta (4–8 Hz) and delta (0.5–4 Hz) bands [1,5]. Since EMD decomposes EEG into oscillatory components ordered by frequency, the first three IMFs primarily capture high-frequency activity. While these initial IMFs may not directly correspond to the pathological low-frequency bands most affected in AD, they nevertheless carry discriminative information related to high-frequency suppression and altered oscillatory patterns in AD. The observed higher performance of EEMD over EMD for 1-minute spectral Topo-maps supports the notion that noise-assisted decomposition better resolves the underlying oscillatory modes, yielding cleaner spectral features that reflect the neurophysiological state of the brain.

Notably, the raw EEG spectral Topo-maps (95.98%) outperformed the EEMD-based spectral Topo-maps (95.60%). This finding highlights the richness of biological information preserved in the raw EEG signal. The close performance gap between raw EEG and EEMD suggests that EEMD acts as a robust noise-resistant alternative rather than a strictly superior representation. This distinction is clinically relevant: in real-world recording environments where signal quality may vary, EEMD-derived features could provide more consistent classification performance. A direct comparison of these two scenarios under noisy signal conditions is a valuable direction for future investigation.

Compared to state-of-the-art methods, our proposed approach achieves competitive accuracy. While Sen *et al.* [12] reported 98.6% accuracy using ITD with time-frequency spectrograms, a key advantage of the present method is the spatial interpretability provided by Topo-maps, which allow clinicians to identify which brain regions exhibit altered activity in AD. The Topo-maps generated in this study (Figures 3 and 4) demonstrate observable spatial differences between AD patients and HC, with notable distinctions in frontoparietal channels, consistent with known patterns of cortical dysfunction in early-stage AD.

Several limitations of this study should be acknowledged. The dataset consists of 26 subjects (15 AD, 11 HC), which is relatively small. The image-level random split used for training and validation does not enforce subject independence, meaning that images from the same subject may appear in both sets. This may inflate reported accuracy relative to a subject-independent evaluation protocol such as leave-one-subject-out (LOSO) cross-validation. Additionally, the results were not validated across multiple independent runs, and no standard deviation or confidence interval is reported, which limits the assessment of statistical robustness. These aspects are acknowledged as limitations and are recommended to be addressed in future work with larger, multi-site datasets.

5. Conclusion

Detection of AD is important in terms of starting treatment as soon as possible and raising an individual's awareness. In this study, detection of AD was done with signal decomposition methods, which are EMD and its variant EEMD, and deep learning. It is aimed to help doctors' judgment as quickly as possible.

In this study, a 2D CNN was used to classify HC and AD. Topo-map were used as input images to the CNN. EMD and EEMD were used to decompose EEG signals into IMFs. Spectral and temporal features were extracted from IMFs (obtained with EMD) and the original EEG signal for 1 min and 5 s cases. Only spectral features were extracted from IMFs (obtained with EEMD) for 1 min cases. These features were transformed into Topo-map. Topo-map give information about the spatial resolution of brain activity across EEG channels for a given feature. They allow for the visualization of which features are more dominant in specific channels for the corresponding signal (such as EEG or IMFs). This spatial perspective adds interpretability to machine learning models by linking features to specific brain regions. These maps help show which brain areas work differently in different groups. Furthermore, researchers can learn more about how brain disorders work by looking at differences in heat maps for different features or conditions. In neurological conditions like AD, these visual comparisons are extremely helpful.

After generating Topo-map, classification of these Topo-maps was performed with ResNet-50, ResNet-18, and EfficientNet-b0 architectures. Spectral features Topo-maps were classified better than time-domain features Topo-maps for 1 min and 5 s cases. In addition, EEG spectral Topo-maps were classified better than IMFs spectral Topo-maps. Classification performance of 1 min IMFs spectral Topo-maps was increased using EEMD. For all architectures, the classification performance of EEMD was higher than that of EMD for 1 min IMFs spectral. For the ResNet-50 architecture, the performance of EEMD is also higher than that of EEG for 1 min spectral case. These results highlight the potential of EEMD as a robust decomposition method for increasing classification accuracy. 96% accuracy was achieved with 1 min EEG spectral Topo-maps as the highest accuracy rate in this study. This high accuracy demonstrates the reliability of spectral features and the effectiveness of the 2D CNN approach in EEG-based AD detection.

In this study, the classification experiments were conducted on a CPU-based computing environment. Although EfficientNet-b0 is an architecturally efficient model designed for fast inference, the large number of Topo-map images generated (over 340,000) resulted in considerable training time. All experiments were completed within a feasible timeframe; however, migration to a GPU-accelerated platform would further reduce training duration. The use of modern deep learning frameworks with GPU support (e.g., CUDA-enabled PyTorch or TensorFlow) is straightforward and is recommended to improve experimental throughput in follow-up studies.

For future work, feature selection can be done to improve the classification performance of IMFs. Other signal decomposition methods, like ITD, Multivariate Empirical Mode Decomposition (MEMD), can be obtained to compare with EMD and EEMD. Also, different features like Logarithmic band power (LBP), Approximate entropy (ApEn), Zero-crossing rate (ZCR), Norm (Norm) can be extracted from the signal. These features can be compared with the features of the proposed study. In addition, the first three IMFs were used in this study. Different combinations of IMFs can be used to find out which IMFs are more successful in classification. As a result, an IMF selection can be made to increase classification performance. After all comparisons between signal decomposition methods, extracted features, and IMFs selection processes, the most effective approach can be learned to classify AD patients.

Data availability statement

The data or datasets that support the findings of this study are available from the corresponding author upon reasonable request.

Declaration of generative AI and AI-assisted technologies

During the preparation of this manuscript, the authors used, such as, ChatGPT, Gemini (generative AI tools) only to improve language and readability, respectively. The authors take full responsibility for the content of the manuscript.

Authors' contribution

Yahya Oguzhan Senol: conceptualization, methodology, software, validation, formal analysis, investigation, resources, data curation, writing—original draft preparation, writing—review and editing, visualization; Aydin Akan: conceptualization, methodology, formal analysis, investigation, resources, writing—original draft preparation, writing—review and editing, visualization, supervision, project administration, funding acquisition; Ozlem Karabiber Cura: conceptualization, methodology, formal analysis, investigation, resources, data curation, writing—original draft preparation, writing—review and editing, visualization, supervision, project administration. All authors have read and agreed to the published version of the manuscript.

Conflicts of interest

Aydin Akan holds the position of Associate Editor for *Electronics and Signal Processing* and has not peer reviewed or made any editorial decisions for this paper.

References

[1] Yu W, Sun T, Hsu K, Wang C, Chien S, *et al*. Comparative analysis of machine learning algorithms for Alzheimer's disease classification using EEG signals and genetic information. *Comput. Biol. Med.* 2024, 176:108621.

[2] delEtoile J, Adeli H. Graph theory and brain connectivity in Alzheimer's disease. *Neuroscientist* 2017, 23(6):616–626.

[3] Jack CR, Bennett DA, Blennow K, Carrillo MC, Dunn B, *et al*. NIA-AA research framework: toward a biological definition of Alzheimer's disease. *Alzheimers Dement.* 2018, 14(4):535–562.

[4] Perez-Valero E, Lopez-Gordo MÁ, Gutiérrez CM, Carrera-Muñoz I, Vílchez-Carrillo RM. A self-driven approach for multi-class discrimination in Alzheimer's disease based on wearable EEG. *Comput. Methods Programs Biomed.* 2022, 220:106841.

[5] Lal U, Chikkankod AV, Longo L. A comparative study on feature extraction techniques for the discrimination of frontotemporal dementia and Alzheimer's disease with electroencephalography in resting-state adults. *Brain Sci.* 2024, 14(4):335.

[6] Tzimourta KD, Afrantou T, Ioannidis P, Karatzikou M, Tzallas AT, *et al.* Analysis of electroencephalographic signals complexity regarding Alzheimer's disease. *Comput. Electr. Eng.* 2019, 76:198–212.

[7] Deng B, Cai L, Li S, Wang R, Yu H, *et al.* Multivariate multi-scale weighted permutation entropy analysis of EEG complexity for Alzheimer's disease. *Cognit. Neurodyn.* 2017, 11(3):217–231.

[8] Mammone N, Ieracitano C, Adeli H, Bramanti A, Morabito FC. Permutation jaccard distance-based hierarchical clustering to estimate EEG network density modifications in MCI subjects. *IEEE Trans. Neural Netw. Learn. Syst.* 2018, 29(10):5122–5135.

[9] Simons S, Espino P, Abásolo D. Fuzzy entropy analysis of the electroencephalogram in patients with Alzheimer's disease: is the method superior to sample entropy? *Entropy* 2018, 20(1):21.

[10] Cura OK, Akan A, Yilmaz GC, Ture H. Detection of Alzheimer's dementia by using signal decomposition and machine learning methods. *Int. J. Neural Syst.* 2022, 250:2250042.

[11] Bairagi V. EEG signal analysis for early diagnosis of Alzheimer disease using spectral and wavelet based features. *Int. J. Neural Syst.* 2018, 10(3):403–412.

[12] Sen SY, Cura OK, Yilmaz, GC, Akan A. Classification of Alzheimer's dementia EEG signals using deep learning. *Trans. Inst. Meas. Control* 2025, 47(7):1353–1365.

[13] Safi MS, Safi SMM. Early detection of Alzheimer's disease from EEG signals using Hjorth parameters. *Biomed. Signal Process. Control* 2021, 65:102338.

[14] Alvi AM, Siuly S, Wang H. A long short-term memory based framework for early detection of mild cognitive impairment from eeg signals. *IEEE Trans. Emerg. Top. Comput. Intell.* 2023, 7(3):724–734.

[15] Fiscon G, Weitschek E, Felici G, Bertolazzi P, De Salvo S, *et al.* Combining EEG signal processing with supervised methods for Alzheimer's patients classification. *BMC Med. Inform. Decis. Mak.* 2023, 23(1):48.

[16] Ieracitano C, Mammone N, Hussain A, Morabito FC. A novel multi-modal machine learning based approach for automatic classification of EEG recordings in dementia. *Neural Netw.* 2020, 123:176–190.

[17] Wan Z, Yang R, Huang M, Zeng N, Liu X. A review on transfer learning in EEG signal analysis. *Neurocomputing* 2021, 421:1–14.

[18] He K, Zhang X, Ren S, Sun J. Deep residual learning for image recognition. *arXiv* 2015, arXiv:1512.03385.

[19] Tan M, Le Q. EfficientNet: rethinking model scaling for convolutional neural networks. *arXiv* 2019, arXiv:1905.11946.

[20] Senol YO, Akan A, Cura OK. Analysis of dementia EEG signals using empirical mode decomposition variants and deep learning. In *Proceedings of the 2025 Medical Technologies Congress (TIPTEKNO)*, Gazi Magusa, Turkiye, October 26–28, 2025. pp.1–4.